CONCEPTUAL DESIGN OF A HIGH-ALTITUDE, LONG-ENDURANCE AERIAL VEHICLE SYSTEM FOR RAPID NETWORK DEPLOYMENT

L. Neveling*, J. Götz†, S. Zoghlami*, S. Dominik†, L. Babetto ‡, E. Stumpf§
* Undergraduate Student, RWTH Aachen University, Germany
† Graduate Student, RWTH Aachen University, Germany
‡ Research Assistant and PhD Student, Institute of Aerospace Systems, Aachen, Germany
§ Head of Institute of Aerospace Systems, Aachen, Germany

Abstract

The preliminary design of an aircraft system for the provision of communication services to disaster-affected regions is presented. Based on two mission scenarios, mission requirements and a design process are defined. A concept is chosen through a trade-off study. The system architecture is outlined, and the TRL of the involved subsystems is discussed. For the detailed design, an initial sizing defines the aerodynamic and propulsive parameters of the aircraft system. Both mission scenarios are fully analyzed. Structural sizing follows after the evaluation of the aerodynamic parameters. Concepts for the operation of the aircraft system and its infrastructure are presented. The aircraft system is holistically evaluated, consisting of a failure probability analysis and a cost analysis. Lastly, the sustainability of the concept is discussed as an increasingly important aspect of aviation.

Keywords
Network Deployment; DLR Design Challenge; HALE Platform

NOMENCLATURE

Abbreviations

A/C	Aircraft
AoA	Angle of Attack
AV	Aerial Vehicle
AVL	Athena Vortex Lattice
CoG	Center of Gravity
DC	Direct Current
DLR	Deutsches Zentrum für Luft- und Raumfahrt
DoF	Degrees of Freedom
EIS	Entry into Service
EU	European Union
FCS	Flight Control System
FL	Flight Level
HALE	High-Altitude Long-Endurance
HAP	High-Altitude Platform
HEIKE	Hochfliegende, effiziente und intelligente Krisenkommunikationseinheit
ILR	Institute of Aerospace Systems
INS	Inertial Navigation System
MSL	Mean Sea Level
MTOM	Maximum Take-Off Mass
NM	Nautical Miles
PMADC	Power Management and Distribution Control
SoC	State of Charge
TCAS	Traffic Alert and Collision Avoidance System
TCR	Technology Compliance Level
TLAR	Top Level Aircraft Requirements
TRL	Technology Readiness Level
UAV	Unmanned Aerial Vehicle

1. INTRODUCTION

1.1. Motivation

The aviation sector faces enormous economic and environmental challenges in the coming years, partly due to climate change. These require innovative and sustainable ideas and approaches in order to offer added value to society. In this context, the German Aerospace Center (Deutsches Zentrum für Luft- und Raumfahrt) has been holding an annual competition since 2017 for students to develop forward-looking aircraft concepts based on current priority topics in aviation research. In recent years, the DLR Design Challenge has covered a wide range of topics, from commercial supersonic transport to small rural aircraft, hydrogen-powered aircraft, parcel drones and firefighting aircraft. Further information on the history can be found in [1].

1.2. Task

Communication via the Internet and mobile radio has become an essential part of modern life. Permanently functioning communication channels are particularly important in crisis and disaster situations, as they facilitate the implementation of relief and rescue missions. However, in the event of a disaster, ground-based internet infrastructure can be destroyed, even with extensive coverage, and this communication channel would not be available in a critical situation. This year's Design Challenge therefore aims to design an aircraft to restore internet coverage over a large area for an extended period of time. In addition to securing this communication path, the aircraft should also be able to quickly create a situation picture of a disaster area. The requirements for efficiency in continuous operation and rapid operational readiness in the event of a disaster are to be combined in an aircraft or system design. The exemplary emergency scenario, which forms the starting point of the design, can be divided into two phases. In the first phase, there is a large-scale and long-term communication and internet failure that affects the federal states of Hamburg and Schleswig-Holstein. The aim is to restore the internet supply as soon as possible. In a second phase, there is also a local and time-critical disaster, which requires reaching the area 170 NM away in less than two hours, as well as Internet restoration and situation monitoring.

1.3. Participants and results

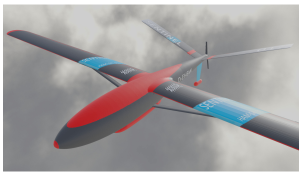

(a) DHBW Ravensburg - The Sentinal System

(b) University of Stuttgart - PERSEUS

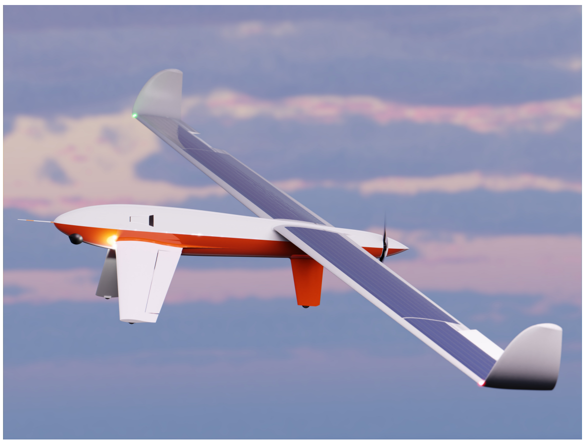

(c) RWTH Aachen University - HEIKE

(d) TU Dresden - AirLive

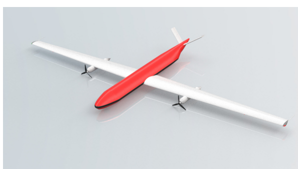

(e) Trier University of Applied Sciences - Prometheus

FIG 1. Overview of all concepts of the DLR Design Challenge 2023

The field of participants in this year's DLR Design Challenge consists of five different teams and a total of 25 students. The following universities are represented: RWTH Aachen University, TU Dresden, DHBW Ravensburg, University of Stuttgart and Trier University of Applied Sciences. The submitted designs feature a wide variety of aerodynamic configurations and drive concepts. Further information on the designs shown in Figure FIG. 1 can be found in the press release [2]. Concept *HEIKE* is presented in detail below.

2. DESIGN PROCESS

In order to develop a suitable system of aerial vehicles, a design process is established, which is schematically shown in FIG. 2. Initially, the task is studied and TLARs are identified. This is followed by a list and ranking of derived evaluation criteria. Five exemplary concepts were developed, which are defined by the solution space from the derived Zwicky Box. An attempt was made to obtain a wide range of solutions in order to identify tendencies and maintain flexibility in the design process. A subsequent pairwise comparison is used to select the best concept, which is initially defined in the initial sizing process, and to identify key parameters for the further design process. A detailed design of the subsystems is then presented, which are subsequently tested in a mission simulation. Findings about the performance are directly fed back into the detailed design step and thus, a holistic evaluation of the flight performance with respect to the required mission is possible. Lastly, the costs for the developed aircraft systems are analyzed, a sustainability analysis is performed. Additionally, multi-use/multi-role capabilities are considered.

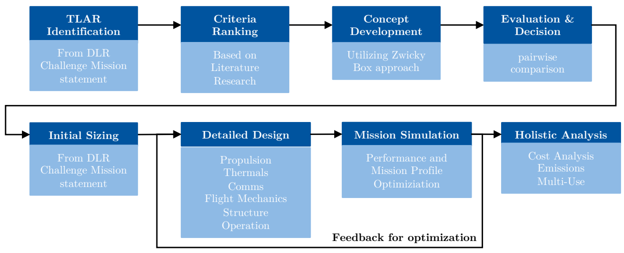

FIG 2. Design Process adapted from [3] [4] [5]

The following criteria represent the key requirements for the final aircraft. **Fast deployment** and **operational readiness** are essential in the event of a disaster, and the time required to prepare the aircraft for take-off is essential. Likewise, **efficiency in continuous operation** must be ensured so that the duration of the mission can be maximized. Short-duration operations contrast sharply with long-duration emergency operations, where **full recovery of critical communications infrastructure** on the ground can take several months. Internet recovery is essential for the affected population and for the situational awareness of the emergency responders. Fail-safe systems with built-in redundancies and energy as well as power backups are of high importance. **Earth observation and sufficient coverage** are defined and must be met with the failure of some units. This requires wisely choosing flight performance parameters, such as service ceiling and cruise speed. Intelligent mission planning and optimized operational strategies for the use of available energy sources and regenerative systems must be used. Eventually, the developed system must be set up, maintained, and used by humans under difficult conditions, *e.g.*, at night or in time-critical emergency situations. This places demands on **easy handling** and requires that the **user experience** is kept in mind throughout the system conceptualization. Resulting design criteria and their respective weighting (applied during the concept evaluation in Section 2.2) are collected in TAB. 1.

2.1. Design Criteria

Criteria	Rank [-]	Weighting [%]
Mass	17	2.16
Emissions	20	0.86
Scalability	18	1.73
Flight duration	4	6.48
Maintenance effort	15	3.45
Cost	22	0.65
System Responsiveness	6	6.26
Transportability	12	4.75
Total System failure rate	1	8.64
Resistance to environmental influences	3	8.20
User Handling	19	1.51
Range/Endurance	6	6.26
Required Infrastructure	14	4.10
Multiuse capability	16	2.59
TRL	20	0.86
Certification compliant	13	4.32
Safety	2	8.42
Launch Distance	10	5.40
Glide ratio	8	6.04
Climb rate	9	5.61
Altitude	5	6.30
Speed	10	5.40

TAB 1. Criteria ranks and weighting

2.2. Concept Analysis and Evaluation

A variety of concepts have been methodically developed using the Zwicky Box, covering the entire solution space to the greatest extent possible. In the selection process, attention was paid to combining various technologies in a meaningful way without limiting each other. The features are summarized in TAB. 2 and design sketches were drawn for visualization, as shown in FIG. 3. A comprehensive analysis was carried out using the pairwise comparison. The following evaluation is only a compact part of the overall concept evaluation.

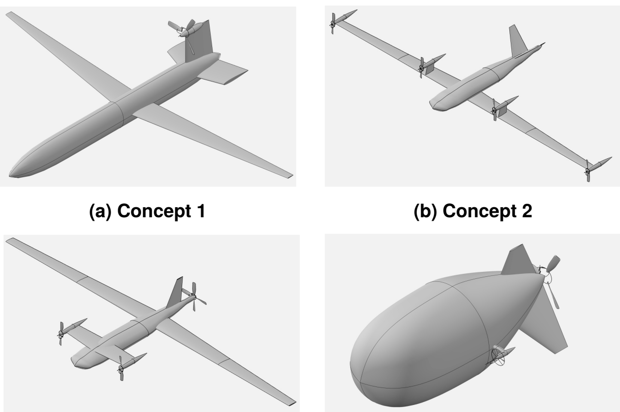

(a) Concept 1 **(b) Concept 2**

(c) Concept 3 **(d) Concept 4**

FIG 3. Proposed concepts, modeled with OpenVSP [6]

No.	Configuration	Average Score	TCR [%]
1	Manned motorized glider, mono-electric propulsion utilizing batteries and solar cells, pull prop, T-Tail, modular/dismountable structure, conventional TO&Landing, hand force control, hangar stored	1.88	37.6
2	Unmanned hybrid-serial propelled, electric motor paired with battery, rotary engine and AvGas, V-Tail, unpressurized fuel tank, pull and wingtip propellers, remote controlled, Fly-by-Wire, conventional TO&Landing, hangar stored	2.91	58.2
3	Unmanned canard/tandem type VTOL capable, mixed hybrid-serial propulsion, battery storage, unpressurized fuel tanks, tiltable rotors and elevator, fully autonomous operation, container stored	3.72	74.4
4	Unmanned Airship, inverted Y-Tail, mono-propulsion with fuel cells, H2 filled, deflatable, push prop (back) and pull prop (lateral fixed), aerostatic lift generation, fully autonomous operation, hangar stored	3.26	65.2
5	Unmanned fixed-wing, Canard/Tandem type, inverted V-Tail with integrated landing gear, STOL capable, hybrid-electric driven, utilizing fuel cells and batteries, solar cells on wing, pushprop with large diameter, fully autonomous operation	4.07	81.4

TAB 2. Evaluation of developed concepts

Concept 1 is not considered due to the necessity of a pilot in the aircraft; in case of pilot incapacitation, total loss of control ensues. Furthermore, the reliance on mono-electric propulsion presents a lack of redundancy in the event of failure of the power supply. The hand-force control further diminishes the handling quality. **Concept 2** reduces the risk of loss of control by having the pilot steer the aircraft remotely. However, the hangar storage limits the flexibility of the concept. Service deployment is limited to regions in the vicinity of the hangar location. This problem is mitigated by opting for a container-storable, for instance, **Concept 3**. Additionally, this concept poses minimal requirements towards the take-off and landing site by incorporating tiltable propulsion elements. A drawback of the innovative *VTOL* (vertical take-off and landing) capability, however, is the increased risk of failure associated with the complexity of the additional subsystems (*e.g.*, propeller actuation). Also, the difference in hover and cruise power requirement does not represent a suitable solution. As a fundamentally different approach, an airship configuration was considered for **Concept 4**. This concept provides several benefits, such as flexibility regarding the launch location, a long airborne phase, and the potential for the spatial separation of components. However, considering that the deployment scenario requires a fast response time, the high cost of Helium, and airspeed make this concept inadequate [7]. Also station-keeping in the wind is not feasible [8]. The final **Concept 5** eliminates all of the above design and operational flaws:

- Autonomous vehicle removes human point of failure.
- Container transportation provides quick and spatially flexible emergency response.
- Hybrid energy source (solar cell and fuel cell) ensures operation independent of weather situation.
- High aspect ratio wings for improved gliding performance and thus long airborne phase.

3. CONCEPT 5: SYSTEM ARCHITECTURE *HEIKE*

In the course of the DLR Design Challenge, the system *HEIKE*, which is the German abbreviation for *Hochfliegende, effiziente und intelligente Krisenkommunikationseinheit* was developed, which meets the mission goals, TLARs and performance specifications listed in TAB. 3. A sketch of *HEIKE* is displayed in FIG. 4.
The combination of a lightweight payload but with a high power requirement over an extended period of time presents a design challenge for this aircraft system. The proposed solution copes with this challenge by using advanced design methods and novel solution concepts as presented in Section 4. Ensuring a continuous operation as well as rapidly and simultaneusly deployable with high coverage,

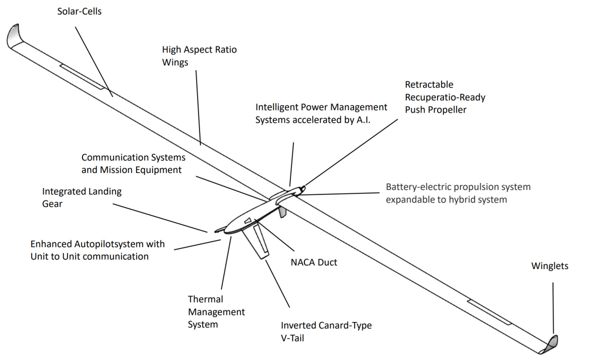

FIG 4. Developed high-altitude aerial platform concept *HEIKE*

poses particular challenges to *HEIKE*. The targeted minimum duration of the design mission is 30 days in the most conservative case with the presented system, as suggested by [9]. This entails:

- Launch in a winter month at the highest latitude (55°)
- Weather: closed cloud layer up to 12 km altitude
- Launch time at 10 a.m. so that a subsequent recharge phase using solar power cannot be relied on due to the early winter break of dusk

A manned system would significantly increase system mass due to required life support systems, *e.g.*, pressurized environment, as well as limit mission time due to human abilities and regulatory work schedules. Accordingly, an autonomous system was chosen because it offers the following advantages: Higher control speed, reproducibility, increased accuracy, lower risk of failure as human errors are reduced, and therefore, higher reliability [10]. In addition, acceleration limits, temperature and pressure limits for unmanned aircraft systems are higher than for manned platforms [11]. The mission posed special requirements to the thermals and power supply as there are different design points for maximum temperature in summer at high latitudes (long days) and simultaneously maximum solar power available, which contradicts thermal cooling power and powertrain power supply. A careful consideration of these factors was made.

Top Level A/C Requirements	Value
MTOM	357.9 kg
Cruise Speed	50 m/s
Deployment Rate	<20 min
Number of required A/C	20
Continuous Operating Time	minimum 30 days
Max. Flight Level	820
Battery Size	56 kWh
Solar Cell Area	25.72 m^2
Max. Climb Rate	4 m/s at MSL
Entry into Service	2040
Take-Off Field Length	<100 m
Glide Ratio	54

TAB 3. Top Level Aircraft Requirements achieved by *HEIKE*

For optimal efficiency in operation, the thrust vector is placed along the x-axis of the body-fixed coordinate system so that no additional torque to be compensated is generated, especially in the loiter phase. Therefore, a push propeller is placed at the tail of the aircraft, which is equipped with a retraction mechanism to minimize drag during the thrustless trimmed night glide phase. Distributed Electric Propulsion is not considered because of undesired propwash effects on aerodynamic surfaces and their negative effect on handling, transportation, maintainability, mass, and cost.
In the coasting phase, the ability to recuperate is not envisioned until the EIS in 2040. There are several reasons for this: The propeller must operate as efficiently as possible at several aerodynamic operating points, for instance, at low altitudes with high air density, at high altitudes with low air density, and at different temperature levels over a longer period of time. Moreover, the propeller has to be designed to be foldable in order to be smoothly transported to the point of use. For reasons of system complexity, integration into the high-voltage electric powertrain would also add higher costs in terms of development and supply. After consideration the trade-off between recovered energy through recuperation and drag created by windmilling, makes this option unfeasible for the performance analysis but will be integrated into the system once the technologies achieve a sufficiently high TRL. *HEIKE*'s system architecture is schematically shown in FIG. 5.

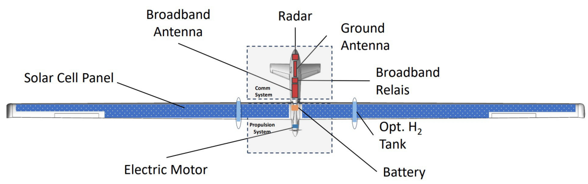

FIG 5. System architecture for proposed *HEIKE* design

Paramount is that continuous deployment of network capabilities and communication systems by *HEIKE* can only be achieved by the future integration of terrestrial, HAPs, and satellite networks in the long-term [12]. As an unmanned HAP, following the example of gliders, thermals play a central role. *HEIKE* exploits the available environment for heating and cooling and uses not only chemical, gravimetric but also meteorological available energy sources like gliders.

3.1. Coverage, Fleet Concept, Operational Readiness, and Multi-Role Design

With its modular design, *HEIKE* is applicable in scenarios beyond the provision of communication services. Other potential customers for the communication services may include passenger airlines, railway operators, cruise ships, and alpine resorts. *HEIKE* may also be used for observational tasks both in the direction of Earth (*e.g.*, wildfire monitoring, agricultural monitoring, and large-scale effects of climate change) as well as at higher altitudes in the direction of the outer space (*e.g.*, research of the upper atmosphere and ozone layer, the possibility of improved conditions for astronomy). It will also demonstrate important technological advances for long-endurance unmanned aerial vehicles to support space exploration, such as in the atmosphere of Mars. In general, the modular payload unit of *HEIKE* allows a wide variety of alternative payloads to be carried.

3.2. Safety Architecture and Certification Requirements

Mission Profile planning needs to be in compliance with air traffic controllers and regulations. EASA's regulation [13] for unmanned aircraft systems are partially applicable.

Regarding autonomous flight operation, sensor fusion, and measurement consolidation ensure safe autonomous operation. High-performance signal processing is included. Emergency systems are integrated into the flight control software, providing various levels of safety. For example, if the pitch damper receives warnings of a failed sensor, the angle of attack is estimated by filtering, and limited authority is used. In case of a total failure of the system, a backup control law via remote control by trained personnel is integrated. This ensures guiding the unit safely to a nearby field for landing and retrieving the failed units, thus, it can be redeployed once the systems are running nominal again. In a gimbal system equipped with various optical measuring instruments, the system can navigate independently. In addition to shielded GPS/GALILEO receivers, Terrain Reference Navigation, and an Image Based Navigation are available.

3.3. Future technologies for EIS 2040 & TRL

The aim of *HEIKE*'s design is to utilize currently available technologies and to provide a solid foundation for its design. In this context, many of the selected components have achieved level 8 or 9 on the TRL scale by 2023 [14]. However, it has always been considered to ensure that *HEIKE* remains a state-of-the-art aircraft upon its introduction in 2040. For this reason, *HEIKE* is not heavily dependent on further development, but it can benefit from advancements such as higher-efficiency solar cells, robust flight control, or lighter structures.
The battery is the most reliant on further development, specifically in terms of energy density at pack level. Currently, energy densities of around 180 Wh/kg are used [15], whereas *HEIKE* requires at least 400 Wh/kg. Obtaining reliable data for future battery technologies is challenging due to the potential for significant breakthroughs like solid-state batteries. Such progress is not guaranteed, but a target of 400 Wh/kg is considered relatively pessimistic compared to other predictions [16]. If these advancements are indeed achieved, *HEIKE* will benefit from increased mass capacity, allowing for a larger battery or higher payload. Based on collected information, the battery is estimated to have a current TRL of 3 to 4 [14].
According to the Unmanned Aircraft System Road map 2005–2030 published by the U.S. Department of Defense [17], the necessary autonomous capability level for *HEIKE*, ranks ninth on a 10-level scale, is expected to be widely achieved by 2030. In the future, the hybrid propulsion system, consisting of both a battery and a fuel cell, should be reevaluated [18, 19]. However, the use is dependent on significant weight reductions in the area of hydrogen storage. Regenerative fuel cells can also be integrated into the proposed system in the long term.
To improve flight performance, *HEIKE* uses morphing wing flaps, thus, an optimal L/D can be achieved in different flight environments [20, 21]. Furthermore, it could be considered to equip *HEIKE* with Lufthansa Technik's *AeroSHARK* [22] to reduce drag. Also, a novel method is used to combine structural components with thermal conduction systems, which will be introduced in Section 4.3 and briefly discussed.

3.4. Technical Drawing of *HEIKE*

FIG. 6, FIG. 7 and FIG. 8 show the Front, Top, and Side-View of *HEIKE*.

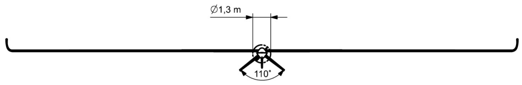

FIG 6. Front View

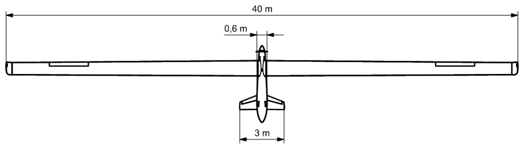

FIG 7. Top View

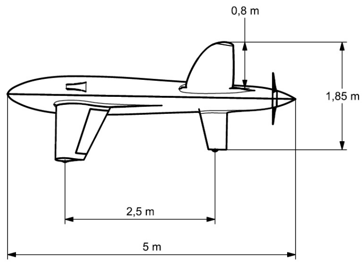

FIG 8. Side View

4. DETAILED DESIGN

In order to design a suitable aircraft system in detail, advanced design and analysis approaches have been used: *Evolutionary algorithms* similar to [23] accelerate the process of finding optimal aerodynamic configurations [24], which are simulated in a *rapid virtual prototyping* process. In this way, it was also possible to obtain a *digital twin* at medium system level [25]. Thus, the design process shown in FIG. 9 was developed. This design process is supported by various built-in tools.

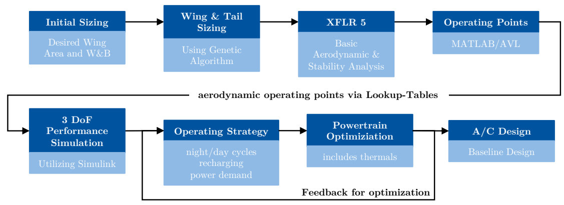

FIG 9. Detailed Design Process utilizing flight dynamics and performance simulation

4.1. Initial Sizing

For the initial sizing, the flight performance requirements are derived from the mission details. Firstly, the requirements for scenario 1 were analyzed. The broadband antenna beam creates a cone, resulting in a round projected area on the ground. However, this poses a challenge because it is not feasible to arrange circles in a manner that covers every bit of land without overlapping. Therefore, the objective is to employ a shape that enables full coverage with minimal overlap. Hence, the hexagon shape was chosen (see FIG. 10). In FIG. 11, the number of aircraft required for area coverage is visualized for the largest possible hexagon and square shape that can fit within the cone.
With regard to speed, two cases are relevant. Firstly, a slow cruise flight at a high altitude is preferred to minimize energy

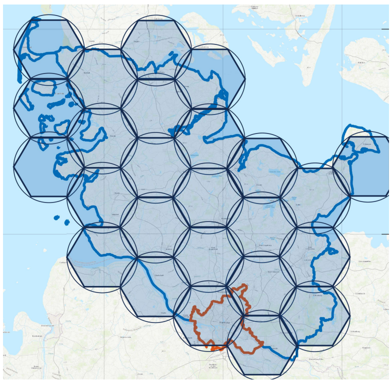

FIG 10. **Full coverage with hexagons**

consumption and reduce the number of aircraft required for scenario 1. Using the diagrams shown in FIG. 11 the cruise altitude was set to 20,000 m. Due to the fact that minimum thrust speed and stall speed are nearly identical for our configuration, a cruise speed of 125 % of the stall speed is selected. Secondly, scenario 2 necessitates a minimum ground speed of 45 m/s at an altitude of 15,000 m.
As shown in FIG. 11, a high service ceiling is necessary to limit the number of aircraft. Furthermore, a service ceiling higher than the cruise altitude allows *HEIKE* to store energy in the form of gravimetric energy. Therefore, a service ceiling of 25,000 m is selected. To quickly cross general aviation airspace, two rates of climbs are determined to 4 m/s at sea level and 2 m/s at cruise altitude. For these requirements, a constrained analysis is carried out with additional functions for the take-off distance and a level turn.

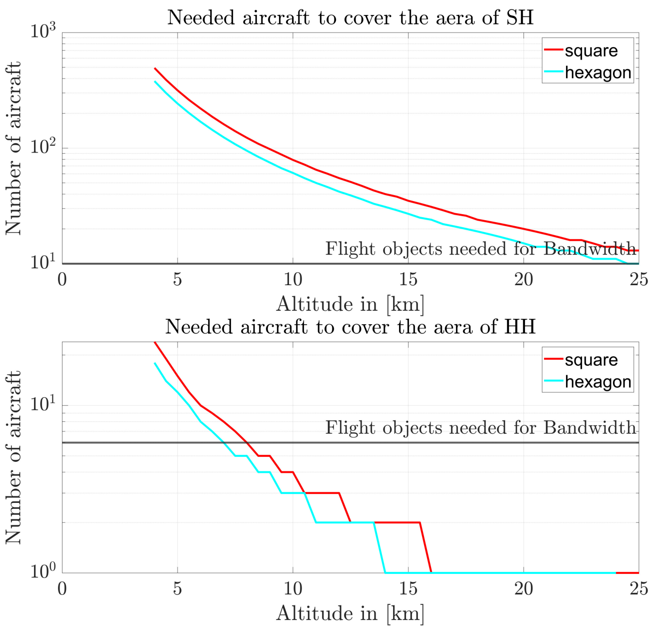

FIG 11. Number of aircraft needed for area coverage: A comparison between square and hexagon

Subsequently, a maximum airspeed-stall speed carpet plot is created for an estimated mass and the power requirements from the constrained analyses. In addition to the speeds for a range of wing surfaces based on the results of the constrained analyses, the propeller efficiency is also calculated based on a blade efficiency of 85 % [3]. This process runs iteratively where the propeller efficiency is used to recalculate the power requirements from the constrained analysis. All calculations shown in FIG. 12 and FIG. 13 are based on Chapter 3 "Initial Sizing" of the General Aviation Aircraft Design [3]. In the early stages of the design process, empirical mass estimations for HALE-UAVs were used for *HEIKE's* fuselage and tail [26]. The wing mass, however, was estimated directly through an idealized structure model featuring a single-cell torsion box [3]. As the design process progressed, these methods were eventually replaced by the structure calculation described in Section 4.4.

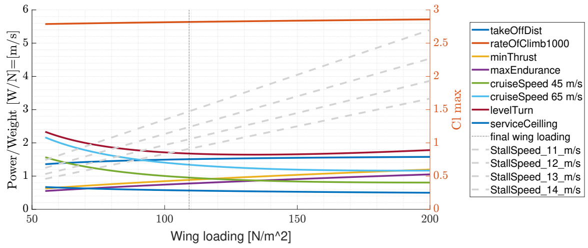

FIG 12. Constrained Analysis

For further calculations, a wing loading of approximately 110 N/m^2 has been chosen. This selection is based on the results in FIG. 12 and represents a trade-off between power consumption at lower speeds and wing mass. Furthermore, the stall speed at cruise altitude remains manageable, as shown in FIG. 13, and the power consumption curve at high speeds shows a clear flattening. Additionally, the required maximum coefficient of lift ($C_{L,max}$) for takeoff is realistically low. Considering these factors, a wing loading of around 110 N/m$\hat{2}$ provides a suitable balance between power consumption, wing mass, stall speed, and takeoff requirements.

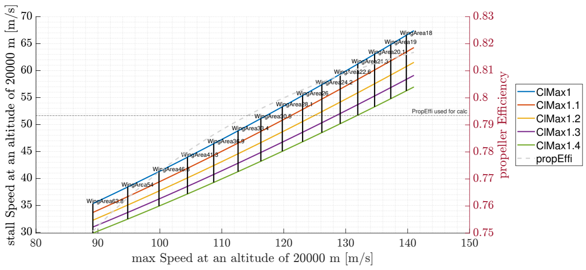

FIG 13. Stall Speed - Cruise Speed Plot

The initial sizing process generates a loop with the flight mechanical design and the powertrain sizing to continuously improve the estimation of aerodynamic coefficients and total mass.

4.2. Aerodynamics, Flight Mechanics, Operating Strategy and Autonomous Systems

In order to be able to make a holistic evaluation of the proposed concept, the self-developed software modules of an aerodynamic analysis by means of utilizing a vortex lattice method *Athena Vortex Lattice* (AVL) [27, 28] as well as XFOIL [29] and a built-in 3DoF simulation environment were combined to investigate the concept. *HEIKE* has control of the longitudinal flight conditions by means of classical PID control [30–33]. Dynamics of the rudder and actuator system as well as thrust actuators were considered. The outer control loop, which includes the mission sequence control, was modeled with finite-state machines. This is done to allow flexible modeling and, in turn, to include optimal operation strategies proposed in [34–36]. Thus, a preliminary Level-D Simulator was achieved according to [37]. Basic aerodynamic performance and stability analysis were first carried out in XFLR 5 [38]. The chosen aerodynamic design ensures that no wings or payload modules reduce solar radiation in level flight. In turned maneuvers, the inverted V-tail maximizes the possible irradiated solar cell area if solar cells would be applied there in future configurations of *HEIKE*.

In addition, the shoulder deck configuration was also selected to avoid shadows on the solar cells during roll maneuvers. Polyvinyl chloride film coatings for improving the aerodynamic performance of solar cell integrated within the upper wing surface and a protection layer against weather conditions or chemicals extends lifetime but decreases the efficiency of the solar cells [39] are being used. In fact, a large camber reduces the possibility of mounting solar cells over a large area without severe bending. For these reasons, the airfoils are of a relatively low camber. The dominant criteria for the selection of the airfoil profiles were indeed the highest possible L/D with a simultaneous minimum moment coefficient, both of which are optimally combined in the corresponding Reynolds number range. With all this considered in combination with the canard configuration [40], the appropriate wing and tail airfoil are as follows: for the wing, a slightly changed *FX63-137* airfoil (maximal relative thickness 12.36% at 34.53% chord, maximal relative curvature 4.87% at 47% chord) was chosen and for the tail, a symmetric *FX71-L-150/30 Wortmann* airfoil is used, both are optimized for the flow regimes of *HEIKE* [41, 42] [43]. The aerodynamic geometry is twisted accordingly for flight characteristics while ensuring spacial distribution for the sensitive payload and high-voltage powertrain components. The aerodynamic performance is shown in FIG. 14. *HEIKE* uses a teardrop shape for the fuselage for higher aerodynamic efficiency but also a semi-monocoque approach to make it fairly easy for manufacturing, Maintenance, Repair, and Overhaul (MRO) and cost-effective.

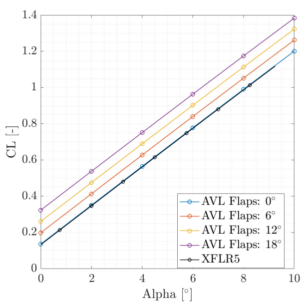

(a) Lift coefficient over AoA

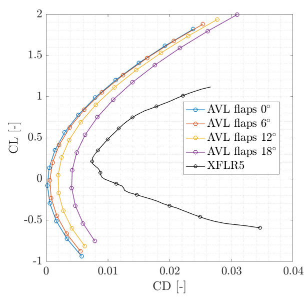

(b) Lift coefficient over drag coefficient

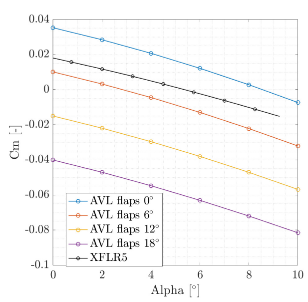

(c) Moment Coefficient over AoA

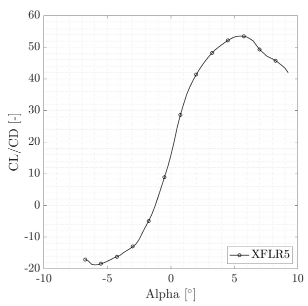

(d) CL/CD over AoA

FIG 14. Aerodynamic performance parameters using [27] [38]

HEIKE's autonomous navigation systems consist of an Inertial Navigation System (INS), which includes three accelerometers, three gyroscopes, a barometric altimeter, and a receiver to the Galileo and GPS network, which is used for support, stability, and drift compensation of measurement data. Other elements include Pitch rate gyro and pitch attitude gyro [10, 44]. Roll rate gyros, yaw rate gyros, and roll attitude gyros are also included. Below the cloud layer, *HEIKE* has a radar altimeter, which is incorporated into the control system through low-pass filters. Additional weather radar in the nose of the aircraft system estimates the weather as well as occurring wind gusts, which operate with combined laser and infrared measurements. In this way, the control system of *HEIKE* can react dynamically to wind speed loads and significantly reduce structural loads through gust load alleviation. Maximum winds occurring at the respective altitudes have been added to the system simulation as a disturbance, and a sufficient stable system response has been found. To mitigate dynamic eigenmodes such as phugoid and short period, *elerudder* (combination of elevator and rudder) deflection controlled by FCS is successfully utilized. The gimbaled system as well as the pitot tube can be seen in FIG. 15.

(a) Optical system gimbal

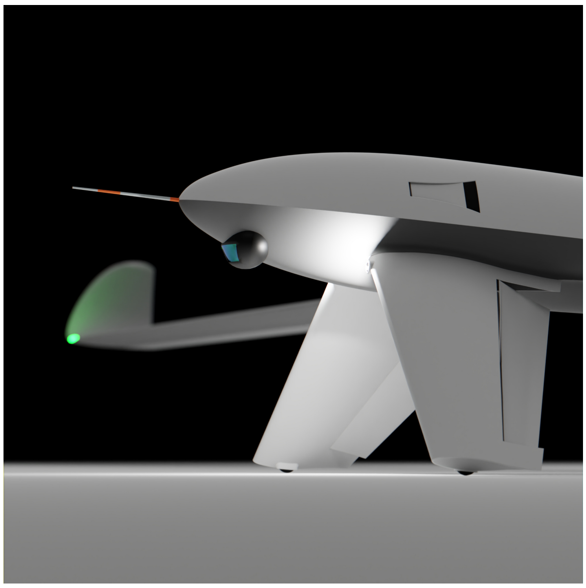

(b) Pitot tube and positioning lights visible

FIG 15. Autonomous Systems of *HEIKE*

Aerodynamic modeling, environmental conditions as well as solar energy models are included in the simulations using modeling techniques from [45, 46]. In the design of control surfaces and control signals within the mission simulation, a limited actuation speed and a load-dependent bandwidth were also taken into account. The rudder hinge does not exceed the critical structural loads according to our results. *FLARM* and TCAS system as well as strobe and position lights to operate in the different airspaces according to the legal regulations are installed in the system. In designing the controller, an elastic structure model is used, which enables the dampening of the structural vibration with the help of notch filters. An automatic controller also enables the generation of set trajectories, calculation of set values such as throttle level, and *elerudder* deflection for the control. A higher level control optimizes the mission strategy in coordination with other *HEIKE* units as well as ground personnel and authorities.

We have chosen a flight mechanically rather unstable design that favors the choice of smaller control surfaces, and lighter structures, as loads are automatically controlled away with powerful control systems [10, 11, 44]. An unstable design provides a range of solutions to the *HEIKE* system: Lift requires a trim tab deflection that results in a lift gain and a simultaneous drag reduction. Maneuvering by changing the lift coefficient results in a supporting moment, thus promoting the maneuver. Gust load alleviation leads to a reduction of structural loads and reduction of maneuver loads for influencing the lift distribution and thereby increasing the structure's lifespan and saving structural weight [10].

The sufficient positioning of the payload antennas during the change of inclination is being compensated with the use of a gimbal system in the internal structure [47]. *HEIKE* is utilizing an intelligent Power Management and Distribution Control System (PMADC) which enables the system to make use of the different energy sources available in an optimal way. Using weather forecast data, wind gusts and internal power states, it will autonomously decide which energy source is best to use. If solar power is available to *HEIKE* during the day, the intelligent PMADC uses this power source to operate the payload and power adjusted according to the current demand to fly the desired trajectory. The excess energy is stored in the battery systems. In this process, the excess energy is also used in such a way that *HEIKE* reaches its service ceiling and thus stores gravimetric energy, which is later converted into kinetic energy during a night phase to save any energy [48]. *HEIKE* also uses thermal circumstances such as winds to exploit additional existing sustainable energy sources. At night, the payload is always provided with the necessary power so that mission success is not affected by external circumstances [9, 39]. A maximum power point tracking device ensures optimal operation of the solar cells.

4.3. Energy System and Thermal Management

When designing the propulsion system, the battery must be able to cope with several load cases. These include the launch phase and the initial long climb to mission altitude. It must then continue to provide power to the payload and store energy for night operations. In addition, the battery must also be able to be recharged in different climatic conditions. The mutual influence between dimensioning the propulsion system and the mission profile results in an optimization problem. A trade-off was made as there are different design points for maximum temperature in summer at high latitudes (long days) and maximum available solar energy, although the temperature of the system must be kept at an acceptable level.

Significant considerations must be made regarding a thermal system, as these represent one of the greatest challenges in the realization of high altitude platforms such as *HEIKE* that are continuously operated [49]. Thermal Management imposes therefore a high risk for failure of the whole HALE system and thus must be addressed. Since at high altitudes heat transfer is no longer primarily dominated by natural or forced convection but by radiation, this must be taken into account in the design of *HEIKE*. The remaining convection must be supported by largely turbulent flow for better-forced convection performance on the suction side and laminar flow on the pressurized side. Phase change materials such as paraffin are a potential solution for the cooling of battery systems, which has already been extensively simulated and tested in the FVA 30 project [50]. Two NACA ducts at the front of *HEIKE* ensure sufficient airflow for the thermal systems and potential turbo-charging capabilities for hydrogen-based fuel cell systems. Also *HEIKE* will be equipped with 3D-printed lattice structures to incorporate new advances in the combined structural and thermal design. It will make use of phase change-material and structural elements shown in FIG. 16b.

As a result of our design method, a battery electric powertrain, which can convert solar energy into electricity through photovoltaic modules, was chosen due to the high efficiency and the required energy demand for our mission. The advantages of a hydrogen-powered drive system outweigh the disadvantages due to the lower system weight and less complexity. Due to the entry into service in 2040, it can be assumed that the fuel cell technology will be more mature, and thus a hybrid concept solution could be possible due to better specific performance data combining another energy source with careful integration into PMADC.

HEIKE is driven by an Axial flux e-motor. The energy source is a 56 kWh lithium-ion battery, which can provide specific energy of 400 Wh/kg through cell-to-pack technology. To charge this battery during flight, 80 % of the wing is covered by mono-crystalline solar cells. For EIS in 2040, the efficiency of photovoltaic modules is expected to improve, which will further reduce the system weight of the powertrain. Efficiency for the solar cells of 14 % is being used inside the performance simulation which gives a good estimate regarding installation losses and pack-level efficiency as well as the temperature sensitivity of the cells. It is important to mention that the scaling of solar modules will also further reduce the purchase price, so it is assumed that the efficiency will increase at the same price.

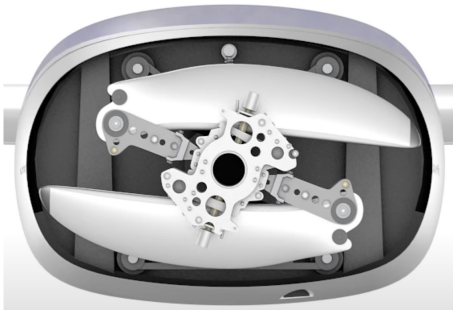

(a) Propeller System of the Stemme S10 [51]

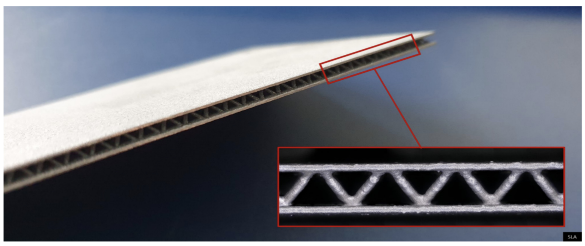

(b) Thermal management structure [52, 53]

FIG 16. Innovative systems in *HEIKE*

To minimize drag during the glide phase, the propeller is equipped with a retraction mechanism that makes use of centripetal force. This system is inspired by the aircraft manufacturer Stemme [51], which already uses this retraction mechanism in the S10. FIG. 16a shows the design of the system.

Detailed results of *HEIKE*'s performance simulation in both scenarios are shown in FIG. 17 and FIG. 18 using a sophisticated flight performance analysis build-in incorporating modeling techniques and methods from [11, 54–62] the use of SIMULINK [25]. Within 164 minutes after launch the target area is reached at 100NM distance from the launch site. *HEIKE* reaches its service ceiling of 20 km within 4 hours and thus the mission of network deployment can be initialized. During the whole mission, the state of charge will never drop below the safety margin of 10 % according to our simulated results. Due to the system design and the choice of cruise speed over ground, *HEIKE* reaches the target area after about 105 minutes in scenario 2. This is a trade-off between the aerodynamic design, the resulting load factors and, accordingly, the structure and propulsion power. Starting with only 75% energy reserve the system exploits the environment thus energy can be recovered, which the operational strategy takes into account. Optional expansion of a hybrid-electric powertrain by adding a regenerative fuel cell can further improve performance.

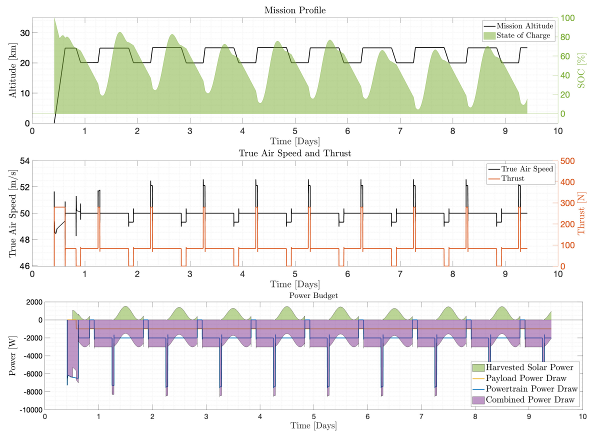

FIG 17. Flight Performance of *HEIKE* for the first 10 days out of a minimum of 30 days of the mission using a 3 DoF- Simulation Framework with integrated aerodynamic operating points

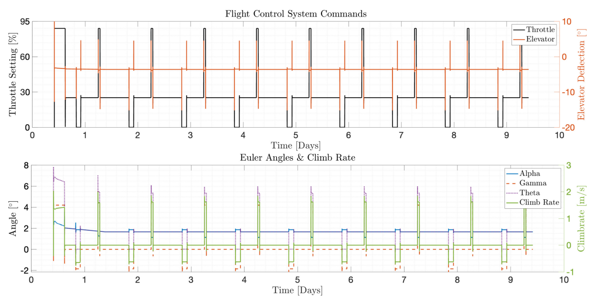

FIG 18. Flight Control System and respective attitudes (Euler Angles) of *HEIKE* for the first 10 days out of a minimum of 30 days of the mission using a 3 DoF- Simulation Framework with integrated aerodynamic operating points

4.4. Structural Design

The structural design here includes the dimensioning of the components of each set of wings (main and V-tail) as well as the fuselage. The design methodology is adapted from Reimerdes [63]. The selected materials were carbon fiber-reinforced polymer for the spars and fiberglass for the wing and fuselage skin. FIG. 19 shows a sectional view with all principal structural components of the wing.

The load cases are calculated from aerodynamic data generated by *Athena Vortex Lattice* [27]. A Matlab function to convert the AVL data to usable load cases was developed. Concerning the wing structural analysis, the load cases are defined by a shear force, a bending moment about the vehicle x-axis, and a torsional moment about the vehicle y-axis. It is assumed that

- the spar caps bear the bending moment.
- the spar sheet bears the transverse (lifting) force and the torsional moment.
- the airfoil bears the torsional moment.

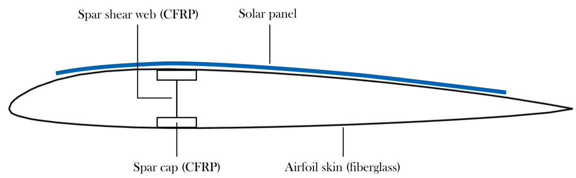

FIG 19. Sectional view of the wing structure

The spar caps are subject to the bending stress

(1) $$\sigma_b = \frac{M(y)\ \frac{H}{2}}{I_{sparcap}}$$

with the area moment of inertia of the spar caps

(2) $$I_{sparcap} = \frac{b}{12}\left(H^3 - h^3\right).$$

The dimension to be sized is the spar cap width b. The spars are placed within the airfoil skin so that the airfoil is divided into two cells of equal cross-sectional area. The shear flow in the airfoil skin can then be calculated with Bredt's formula:

(3) $$\tau = \frac{T(y)}{2\ A_{cross-section}\ t_{skin}}$$

The spar sheet (located between the two spar caps) is subsequently dimensioned to limit the shear stress from both the torsional moment and the transverse force below the maximum shear stress of CFRP. Each component is dimensioned accordingly at discrete spanwise locations. With this methodology, a locally optimized geometry is achieved. Using a gust load factor of 2.5 and a safety factor of 1.75, a lightweight wing design with a total mass of 136 kg is achieved.

The fuselage wall thickness is dimensioned to prevent shell buckling. As a conservative estimate, a simple cylindrical shell without stiffeners is assumed. The principal load acting on the fuselage is the combined bending moment resulting from the aerodynamics at the main and tail wing. First, the bending stress is calculated in analogy with Equation (2). Then, the fuselage wall strength is sized to satisfy

(4) $$\sigma_{cr} = 3.92 E_{fiberglass}\left(\frac{t_{fuselage}}{R}\right)^{1.54}.$$

For the given loads, a fuselage wall thickness of 2.2 mm is sufficient, resulting in a fuselage shell mass of 40.8 kg. It is to be expected that significant mass savings can be achieved with a stiffened shell design.

4.5. Communication and Connectivity, Data Management and Environmental Protection

The communication subsystem is a crucial aspect of *HEIKE*, as it is required to fulfill two roles: The provision of communication services to the affected area, and the data exchange with the ground infrastructure.
A critical design constraint for the communication system is posed by the close proximity to high-voltage components of the energy supply subsystem. These high-voltage components (*e.g.*, inverter, and DC-DC converter) are a source of Electromagnetic Interference (EMI). EMI is an umbrella term for the adverse effects caused by the electromagnetic waves radiated from the high-voltage components, such as induced electric currents, which in turn produce noise in the raw data. Two design options are feasible to reduce the intensity of the EMI at critical components:

- Spatial separation of high-voltage components from communication & data components.
- Enclosure of EMI sources in a Faraday cage.

As spatial separation is limited to the length of the fuselage, the Faraday cage is the appropriate option for this scenario. Nonetheless, it is proposed to additionally maximize the spatial separation by placing all high-voltage components towards the rear of the aircraft (near the electric motor and the power-generating solar) and the communication components towards the front. Concerning the Faraday cages, which are to enclose the inverter and the DC-DC converter, copper mesh is a highly effective EMI shielding material, which allows for a lightweight and failure-proof shielding concept.
The constant provision of communication services is a key requirement. Flight maneuvers may sporadically interrupt the connection. To mitigate this issue, all relays and antennas are flexibly mounted on gimbal joints. The actuation is provided in two rotation axes (about the x-and y-axes of the body-fixed reference system) using two linear electric servo motors per gimbal. A constant pointing of the antenna beam is enabled by feeding data from the autonomous flight computer to the gimbal actuation. Any yaw, pitch, or roll maneuvers are relayed to the gimbal control so that the rotation is instantly compensated.
Aside from rotational maneuvers, the antenna pointing also needs to compensate for the translational motion of the aircraft. The input data for this gimbal motion is extracted from the relative position, altitude, and heading relative to the targeted area. The position can in any case be provided by a navigation satellite system, such as GPS or GALILEO; if multiple ground stations are in service, additional telemetry data may be triangulated from the transmission distance to two or more ground stations. Heading is provided by a compass. Altitude may be provided by a barometric altimeter, with added triangulated data if possible.

4.6. Weight and Balance

An accurate understanding of Weight and Balance, as shown in TAB. 4, is crucial for the entire design process as it influences the flight mechanics, flight performance, and structural sizing of the aircraft. The masses of the structural components are calculated as described in Section 4.4, but their weights are heavily dependent on the masses located in the fuselage. The propulsion system, specifically the battery which weighs 140 kg, constitutes the largest portion of the non-structural masses.

Component	Mass [kg]	CoG x [m]
Payload	13.0	1.0
Propulsion System	157.0	3.5
Autopilot /Flight Systems	2.6	2.5
Landing Gear	0.7	1.8
Fuselage	40.8	2.5
Wing	136.0	3.4
V-Tail	5.8	1.2
Vertical stabilizer	2.0	3.5
EW	344.9	3.3
MZFM/MTOM	357.9	3.2

TAB 4. Weight and Balance of *HEIKE*

Notably, the weight of the battery is dependent on further development, unlike the other components of the flight control and propulsion system, where the masses are based on currently available options. This approach is adopted because it was challenging to obtain reliable estimates for the masses of these components in the future. Furthermore, compared to the battery, the other masses are relatively light, implying that further developments resulting in lighter options would have minimal impact on the overall system.
In the case of *HEIKE*, the maximum zero fuel mass (MZFM) is equivalent to the maximum takeoff mass (MTOM). This is because *HEIKE's* only energy storage comes from the battery, and the mass change of the battery between full and empty is considered negligible. The Weight & Balance of *HEIKE* is visualized in FIG. 20.

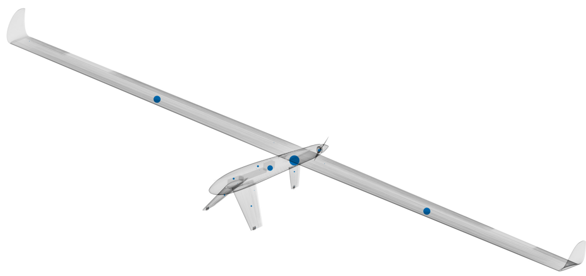

FIG 20. Weight and Balance visualization

4.7. Reliability, Maintainability, Supportability, and Transportability

As an emergency response aircraft system, fast and easy use is vital for an effective operation. The key for our strategy is *HEIKE's* specially designed storage unit that is identical in its dimensions and pickup points to a 40-feet shipping container. Thus, every vehicle that is capable of transporting containers can carry *HEIKE*. This is a significant advantage since the logistics network for containers already exists. Therefore, worldwide transport is cheap and without any special permits possible. Additionally, it does not need to rely on one single transport infrastructure during a crisis [64].

The storage units are mainly located at a logistics hub with good access to rail, ship, and motorway. In addition, individual *HEIKE*-Systems are located at airfields throughout Germany, creating a network similar to the rescue helicopter network in Germany [65]. Thus, *HEIKE* can be involved in small operations without any major logistical effort, or the local system can already be deployed while the main fleet is still in transit for larger operations.

To ensure a quick response time, the container is equipped with solar panels on its top. This way, *HEIKE's* batteries are always charged. When the units are stacked, connecting cables are used to provide power to the lower units as well. Alternatively, other power supplies can be connected as needed.

When the container arrives at the mission airfield, *HEIKE* needs to be rigged, similar to a glider. Due to the large span width, the wings are stored in shorter sections, which fit the container size. Each wing is split at the halfway mark. To facilitate quick (dis-)assembly, the selected design at this interface is realized by a bolt spring mechanism. The operating principle to create a safe connection point between the fuselage and the wing is inspired by concepts used by established glider manufacturers who have been implementing this system for a long time. In order to increase work safety and minimize possible errors, rigging aids are used. Redundant sensors are installed at all separation points enabling, together with the autonomous flight system, a comprehensive automatic function check. This, coupled with the rigging aids, facilitates the swift rigging of *HEIKE* even by personnel with limited training.

The number of moving parts is minimized to ensure low maintenance requirements. To achieve this, the servos for the rudders are directly mounted onto the rudders and can be easily accessed through maintenance hatches. Additionally, the payload and propulsion system can be separately replaced as complete packages. This design facilitates ease of work on the systems, reduces the likelihood of errors related to plugs, and enables faster maintenance by swiftly swapping to refurbished systems. Moreover, the storage unit is equipped with a built-in lifting table to assist in moving heavy components, such as batteries.

4.8. Infrastructure, Launch, Recovery Elements, and Ground Elements

The *HEIKE* system depends only on a very small infrastructure. This ensures rapid and flawless operational readiness. Although an airfield would be desirable as a base of operations, *HEIKE* can operate as long as a sufficiently large, paved area is available. This is aided by *HEIKE's* short takeoff and landing capabilities (STOL) [66].

The concept for the ground station involves a main control unit that utilizes a standard 20-foot shipping container as its base. During normal operation, the mission is monitored in the main control unit, which provides the interface for mission adjustments. In the event of an autopilot failure, the main control unit provides three remote controls to take over command of *HEIKE*. Additional modules, such as crew quarters or an energy generator, can be added to the main control unit depending on the infrastructure available at the ground base. These additional modules are also container-based. However, it is worth noting that the ground station can also be powered by the grid or the solar panels on *HEIKE's* transport units. This provides flexibility in terms of power sources for the ground station operation, especially during crises. A conceptual visualization of the described systems is shown in FIG. 21. For further flexibility of the ground operation, the battery can be charged when it is integrated into the aircraft and when it is removed. This enables an optimal charging experience depending on the chosen option.

FIG 21. Conceptual visualization of *HEIKE*'s airfield-based charging equipment and transportation container

5. HOLISTIC EVALUATION

For a successful concept, other aspects must be taken into consideration, including economic and ecological factors. In the case of emergency response vehicles, cost plays a significant role, as high reliability often comes with high expenses. This is problematic because emergency vehicles are typically utilized at a relatively low rate, as they are primarily reserved for emergency situations. As described in Section 3.1, *HEIKE* has numerous potential applications during non-emergency use. Nevertheless, a carefully made cost and failure analysis is still necessary for long-term planning.

Moreover, ecological influences should also be considered, taking into account the environmental impact of *HEIKE's* operation, energy sources, and overall sustainability.

5.1. Failure Probability Analysis

A fault tree analysis [67] has been conducted to identify high-risk failure sources specifically for mission abort scenarios. It is important to underline that this type of analysis differs significantly from an analysis conducted for a total loss of *HEIKE*. For example, a hardware failure in the relay is unlikely to result in a crash but would inevitably lead to a mission abort. Although there is no data at the moment to actually calculate the probability of mission abort, the analysis gives a good overview of critical components and systems. One of the most critical systems is the power supply, shown in FIG. 22. This system is critical not only because all other systems depend on it, but also because of the lack of redundancy during the climb phase. To overcome this problem, the proposed hydrogen system could be advantageous. One possibility is to integrate the entire hydrogen system into a wing pod. This approach has the advantage of requiring only data and high-voltage cables in the wings, which adds little to the complexity of the rigging compared to hydrogen lines. In addition, the wingpod could be equipped with a parachute, allowing the hydrogen system to be jettisoned if the fuel cell becomes ineffective due to thin air or an empty hydrogen tank. If properly sized, *HEIKE* could reach altitudes above cloud level before the wingpod is jettisoned, allowing the solar cells to continue to provide power.

5.2. Cost Analysis

For the cost analysis, the Eastlake Business model was chosen, which can be found in Gudmundsson [3]. Various as-

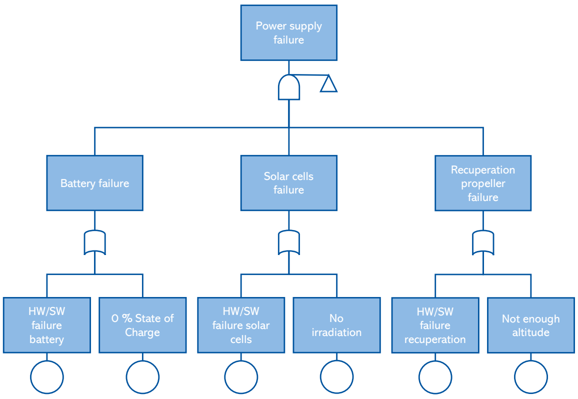

FIG 22. Fault tree analysis: Power supply

sumptions and corrections are made in order to be able to present an actual result. These include, for example, a price level correction through a CPI (Cost Price Index) adjustment, the so-called Cost Escalation Factor (CEF), which is calculated as shown below:

$$CEF = \frac{CPI(\text{now})}{CPI(2012)} \tag{5}$$

In Gudmundsson [3], reference is made to the year 2012, when the CPI of Germany was 91.7 according to statistica [68]. The CPI in 2022 was 110.2, resulting in a CEF of 1.202. In order to obtain a tailored result, the following properties were selected:

- The number of aircraft to be produced within 5 years was set to 200. It should be noted that an increase in the number of aircraft produced has a positive impact on the cost structure due to economies of scale.
- The aircraft does not have a complex flap system.
- The aircraft structure is made of carbon fibre.
- The aircraft does not have a pressurized cabin.
- For the powertrain model, the model has to be adjusted to include an electric powertrain.

Concerning the cost model of the powertrain, a specific cost factor of 200 €/kWh was assumed, which results in a cost of 11.200€ for the selected battery (56kWh). The electric motor is estimated at a cost of 2,000 €. Mono-crystalline solar cells were selected, which have a specific cost factor of approximately 10,000 €/m^2. This cost analysis takes into account that 80 percent of the wing area (32.15 m^2) is covered by cells, the cost equals 257,200 €. Summing up the different cost points, an amount of 270,400 € is obtained.
The currency was changed to Euro and the experience effectiveness was set to 95 percent which results in a Quantity Discount Factor QDF of 0.6757 as calculated by

$$QDF = F_{\text{exp}}^{1{,}4427 \cdot ln(N)} \tag{6}$$

with F_{exp} the experience effectiveness and N the number of units produced.
The detailed cost analysis is shown in TAB. 5.

TAB 5. Cost Analysis

	Work-hours	Rate. €/hr	Total Cost	Cost per Unit
Engineering	11.621,83	100,00	2.928.630,85 €	14.643,15 €
Development Support			82.111,36 €	410,56 €
Flight test operations			293.946,56 €	1.469,73 €
Tooling	21208,84002	61	1.554.744,43 €	7.773,72 €
Certification Cost			4.859.433,20 €	
Manufacturing labor	141061,0293	53	18.839.652,88 €	94.198,26 €
Quality control			1.836.866,16 €	9.184,33 €
Materials/equiment			1.718.429,47 €	8.592,15 €
Units produces in 5 years				200
Quantity Discount Factor				0,6757
			Without QDF	With QDF
Fixed landing gear discount			- 7.500,00 €	- 5.067,75 €
Engine			270.400,00 €	182.709,28 €
Propeller			3.779,49 €	2.553,80 €
Avionics			15.000,00 €	10.135,50 €
TOTAL COST TO PRODUCE			417.951,40 €	326.602,74 €
Manufacturer`s liability insurance				50.000,00 €
MINIMUM SELLING PRICE				376.602,74 €

The cost analysis shows that the minimum selling price for a design of 200 aircraft is 376,602.74€.

5.3. Break Even Analysis

The break-even analysis is used to calculate how many units must be produced before revenues cover costs. With Equation (7), one is able to calculate the number of units to break even.

$$CEF = \frac{\text{total fixed cost}}{\text{unit sales price} - \text{unit variable cost}} \tag{7}$$

FIG. 23 shows the break-even point plotted as a function of units. The cost analysis was designed for 200 aircraft being produced in 5 years. If the price of the aircraft is increased, the number of aircraft needed to reach the break-even point is reduced.

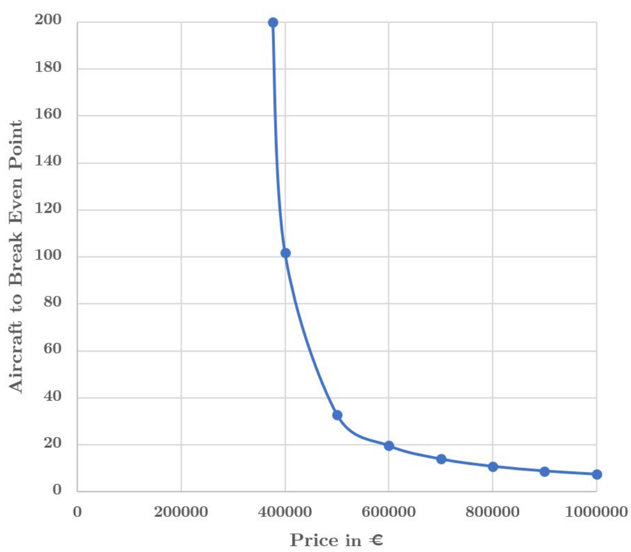

FIG 23. Break-Even Point Analysis

FIG. 24 shows the break-even analysis graphically for 3 different prices. The grey curve represents the minimum selling price. The dark blue curve includes a margin of 5 percent, and the light blue curve has a margin of 15 percent. Furthermore, one can extract, for example, the *Net Present Value* (NPV) at a price of 395,432.88€.

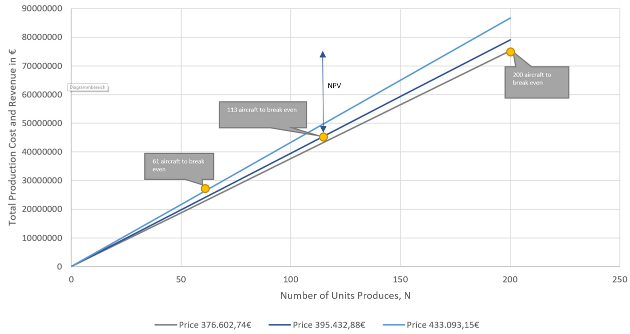

FIG 24. Break-even analysis assuming three different prices

5.4. Environmental sustainability

Sustainability is an important aspect and has been considered throughout the design process. The overall impact is analyzed in the three life stages of production, operation, and end of service.

For the structural components, the main emissions during production are from the autoclave, which is needed to give the CFRP its strength. However, systems are being developed to replace conventional heating elements with microwaves, which should lead to a significant reduction in energy consumption [69]. Similarly, the production of silicon for solar panels requires a lot of energy. The battery, with its high demand for Rare Earth Elements (REE) and energy, currently has the greatest environmental impact. The amount of research into more sustainable solutions is enormous, hence the potential of a more environmentally friendly production process is high. Overall, the industry is expected to have a lower carbon footprint in the future as a result of high investments in renewable energy and thus an increasing amount of green energy in the power grid.

Carbon-neutral operation is possible due to the container design of the storage unit and the electric propulsion system. Rail transport already uses carbon-neutral energy [70], and other forms of transport, such as ships and trucks, are expected to have green options by 2040. The solar cells on the container can charge *HEIKE's* battery for deployment and then power the ground station. During flight, the high aerodynamic efficiency combined with the electric propulsion system minimizes noise pollution.

At present, there are only limited possibilities for recycling an electric aircraft in composite construction. However, with more and more mass-produced products being built in a similar way, e.g., electric cars, the need for a recycling solution for these components is likely to arise sooner than the first *HEIKE* systems are phased out. To support this argument, the EU is already discussing new recycling regulations with the aim of recycling 90 % of batteries by 2030 [71]. Therefore, there should be recycling options for the battery by 2040. CFRP is also difficult to recycle, but the hull is expected to have a long life due to its aerodynamic efficiency (Section 4.2 & Section 4.4) and the ability to replace technical components with newer equivalents [72–74].

6. CONCLUSION AND OUTLOOK

Essential aspects of the mission scenarios were laid out and a design process for *HEIKE* was devised accordingly. An unmanned canard configuration with a pushprop with power supplied by a battery system, later expandable to a hybrid-electric system, was selected for further development. The concept was evaluated regarding the future development of the required technologies, highlighting the energy density of the battery as a crucial parameter. To begin the detailed design, an initial sizing with the power consumption and flight dynamic behavior as trade-off parameters was performed. An unstable configuration was favored over a stable one to reduce the control surface area. The resulting aerodynamic model was used for a full-mission analysis of two emergency scenarios, which demonstrated that *HEIKE* is capable of multi-day missions without the need for landing. For the thermal protection of the battery, the use of phase-change materials as well as 3D-metal-printed lattice structures was proposed. Structural elements were dimensioned with loads obtained from the flight dynamic calculations. The integration of the communication equipment was described, with the final design containing Faraday cages around EMI sources. The detailed design was finalized with concepts for the infrastructure and operation. Operational flexibility was enhanced by making the aircraft system transportable by container. The design was then evaluated for failure probabilities and financial viability. It was shown that the price-per-unit is affordable for a fleet size of 200.

The result is a preliminary design for an aircraft system that is able to provide communication services to disaster-affected regions. Two major challenges are identified for the further roadmap of *HEIKE*: The lightweight design of the power supply, and the coordination of multiple aircraft in autonomous flight. At the time of writing, the available battery technology results in a high battery mass to meet the power demands of the aircraft system. With the global shift from fossil fuels to renewable energies across all industries, research interest in the area will remain high. As for autonomous coordination, research interest is similarly high in comparable areas of application, such as autonomous driving. This ongoing development, coupled with the rapidly growing field of artificial intelligence, will favorably impact the development of *HEIKE*'s autonomous flight system. The design is innovative insofar as it is a novel approach to the mission scenario, which to date has mostly been attempted via satellite networks. However, taking into account the targeted entry-into-service, it is anticipated that all required technologies will be at a serviceable level of readiness by 2040.

Contact address:

johannes.goetz1@rwth-aachen.de

References

[1] DLR Design Challenge. https://www.dlr.de/de/karriere-und-nachwuchs/angebote-fuer-studierende/dlr-design-challenge. [Online; accessed 13-September-2023].

[2] Studierende entwerfen Flugzeug zur Wiederherstellung der Internetversorgung bei Katastrophen. https://www.dlr.de/de/aktuelles/nachrichten/2023/03/the-sentinel-system-gewinnt-dlr-design-challenge-2023, 2023. [Online; accessed 13-September-2023].

[3] Snorri Gudmundsson. *General Aviation Aircraft Design*. Elsevier, 2014. ISBN: 978-0-12-397308-5. DOI: https://doi.org/10.1016/C2011-0-06824-2.

[4] Bernhard Fleischer and Hans Theumert. *Roloff/Matek: Entwickeln Konstruieren Berechnen*. Springer, 2018. ISBN: 978-3-658-22747-0. DOI: https://doi.org/10.1007/978-3-658-22747-0.

[5] *VDI 2221 - Methodik zum Entwickeln und Konstruieren technischer Systeme und Produkte*. Verein Deutscher Ingenieure, 1993.

[6] NASA. OpenVSP. https://openvsp.org, 2023.

[7] Lewis Jamison, Geoffrey S Sommer, and Isaac R Porche III. High-Altitude Airships for the Future Force Army, 2005.

[8] T. C. Tozer and D. Grace. High-altitude platforms for wireless communications. *Electronics and Communication Engineering Journal*, 13:127–137, 2001. ISSN: 09540695. DOI: 10.1049/ecej:20010303.

[9] Yasim J. Hasan, Mathias S. Roeser, Martin Hepperle, Steffen Niemann, Arne Voß, Vega Handojo, and Christian Weiser. Flight mechanical analysis of a solar-powered high-altitude platform. *CEAS Aeronautical Journal*, 14:201–223, 1 2023. ISSN: 18695590. DOI: 10.1007/s13272-022-00621-2.

[10] Univ.-Prof. Dr.-Ing. Dieter Moormann. *Flugregelung Vorlesungsskript*. Institut für Flugsystemdynamik, RWTH edition, 2022.

[11] Reg Austin. *Unmanned Aircraft Systems*. Wiley, 2010.

[12] Abbas Mohammed, Asad Mehmood, Fotini Niovi Pavlidou, and Mihael Mohorcic. The role of high-altitude platforms (HAPs) in the global wireless connectivity. *Proceedings of the IEEE*, 99:1939–1953, 2011. ISSN: 00189219. DOI: 10.1109/JPROC.2011.2159690.

[13] EASA. Easy Access Rules for Unmanned Aircraft Systems — Revision from September 2022, 2022. http://eur-lex.europa.eu/,.

[14] U.S. Government Accountability Office. Technology Readiness Assessment Guide. *GAO Best Practices*, January 2020.

[15] Hendrik Löbberding, Saskia Wessel, Christian Offermanns, Mario Kehrer, Johannes Rother, Heiner Heimes, and Achim Kampker. From cell to battery system in BEVs: Analysis of system packing efficiency and cell types. *World Electric Vehicle Journal*, 11:1–15, 12 2020. ISSN: 20326653. DOI: 10.3390/wevj11040077.

[16] Asep Suryatna, Indah Raya, Lakshmi Thangavelu, Firas Rahi Alhachami, Mustafa M. Kadhim, Usama S. Altimari, Zaid H. Mahmoud, Yasser Fakri Mustafa, and Ehsan Kianfar. A Review of High-Energy Density Lithium-Air Battery Technology: Investigating the Effect of Oxides and Nanocatalysts. *Journal of Chemistry*, 2022, 2022. ISSN: 20909071. DOI: 10.1155/2022/2762647.

[17] Office of the Secretary of Defense. Unmanned Aircraft Systems Roadmap 2005-2030, 2005.

[18] Kangwen Sun, Ming Zhu, Lifeng Wang, and Hu Liu. Analysis of the Hybrid Power System for High-Altitude Unmanned Aircraft. *Advances in Materials Science and Engineering*, 2015, 2015. ISSN: 16878442. DOI: 10.1155/2015/380708.

[19] Ralf Peters. *Brennstoffzellensysteme in der Luftfahrt*. Springer-Verlag Berlin-Heidelberg, 2015. ISBN: 9783662467978. DOI: 10.1007/9783662467985.

[20] Vasile Prisacariu, Mircea Boscoianu, and Ionică Cîrciu. Morphing wing concept for small UAV. *Applied Mechanics and Materials*, 332:44–49, 2013. ISSN: 16609336. DOI: 10.4028/www.scientific.net/AMM.332.44.

[21] Rosario Pecora. Morphing wing flaps for large civil aircraft: Evolution of a smart technology across the Clean Sky program. *Chinese Journal of Aeronautics*, 34:13–28, 7 2021. ISSN: 10009361. DOI: 10.1016/j.cja.2020.08.004.

[22] Lufthansa Technik AG. Lufthansa Technik Aeroshark. https://www.lufthansa-technik.com/en/aeroshark, 2023. [Online; accessed 09-July-2023].

[23] Abu Bakar, Li Ke, Haobo Liu, Ziqi Xu, and Dongsheng Wen. Design of low altitude long endurance solar-powered UAV using genetic algorithm. *Aerospace*, 8, 8 2021. ISSN: 22264310. DOI: 10.3390/aerospace8080228.

[24] Bryan Morrisey and Rob McDonald. Multidisciplinary design optimization of an extreme aspect ratio HALE UAV. 2009. ISBN: 9781563479809. DOI: 10.2514/6.2009-6949.

[25] MathWorks. Matlab/Simulink 2023a. https://de.mathworks.com, 2023.

[26] Zhang Yi and Wang Heping. A Study of Structure Weight Estimating for High Altitude Long Endurance (HALE) Unmanned Aerial Vehicle (UAV).

[27] Mark Drela. Athena Vortex Lattice. https://web.mit.edu/drela/Public/web/avl/, 2023.

[28] Vittorio Cipolla, Andri Dine, Andrea Viti, and Vincenzo Binante. MDAO and Aeroelastic Analyses of Small Solar-Powered UAVs with Box-Wing and Tandem-Wing Architectures. *Aerospace*, 10, 2 2023. ISSN: 22264310. DOI: 10.3390/aerospace10020105.

[29] Mark Drela. XFOIL. https://web.mit.edu/drela/Public/web/xfoil/, 2023.

[30] Robert C. Nelson. *Flight Stability and Automatic Control*. WCB/McGraw Hill, 1998. ISBN: 0070462739.

[31] Task Group SCI-026. Flight Control Design-Best Practices, 2000.

[32] Peter Kämpf. *Handbuchmethoden zur Leistungsabschätzung*. 2022.

[33] Univ.-Prof. Dr.-Ing. Dieter Moormann. *Flugdynamik Vorlesungsskript*. Institut für Flugsystemdynamik, RWTH edition, 2020.

[34] Mou Sun, Chuan Shan, Kang Wen Sun, and Yu Hong Jia. Energy Management Strategy for High-Altitude Solar Aircraft Based on Multiple Flight Phases. *Mathematical Problems in Engineering*, 2020, 2020. ISSN: 15635147. DOI: 10.1155/2020/6655031.

[35] Xian Zhong Gao, Zhong Xi Hou, Zheng Guo, Xiao Qing Chen, and Xiao Qian Chen. Joint optimization of battery mass and flight trajectory for high-altitude solar-powered aircraft. *Proceedings of the Institution of Mechanical Engineers, Part G: Journal of Aerospace Engineering*, 228:2439–2451, 11 2014. ISSN: 20413025. DOI: 10.1177/0954410013518510.

[36] Steve Chukwuebuka Arum, David Grace, Paul Daniel Mitchell, Muhammad Danial Zakaria, and Nils Morozs. Energy management of solar-powered aircraft-based high altitude platform for wireless communications. *Electronics (Switzerland)*, 9, 1 2020. ISSN: 20799292. DOI: 10.3390/electronics9010179.

[37] Federal Aviation Administration. AC 120-40B - Airplane Simulator Qualification, 1991.

[38] DLR. *XFLR 5*. GNU General Public License, 2023.

[39] Magdalena Peciak, Wojciech Skarka, Krzysztof Mateja, and Maik Gude. Impact Analysis of Solar Cells on Vertical Take-Off and Landing (VTOL) Fixed-Wing UAV. *Aerospace*, 10:247, 3 2023. ISSN: 22264310. DOI: 10.3390/aerospace10030247.

[40] Yu Cai, Jiacheng Xie, Evan D. Harrison, and Dimitri N. Mavris. Assessment of Longitudinal Stability-and-Control Characteristics of Hybrid Wing Body Aircraft in Conceptual Design. American Institute of Aeronautics and Astronautics Inc, AIAA, 2021. ISBN: 9781624106101. DOI: 10.2514/6.2021-2448.

[41] Safyanu Bashir Danjuma. Aerodynamic Design Consideration for Stability of a Lightweight Solar-Powered Aircraft. *Traektoriâ Nauki = Path of Science. 2022*, 8, 2022. ISSN: 2413-9009. DOI: 10.22178/pos.81-10.

[42] Mohammad Sakib Hasan, Jelena M Svorcan, Aleksandar M Simonović, Nikola S Mirkov, and Olivera P Kostić. Optimal Airfoil Design and Wing Analysis for Solar-Powered High-Altitude Platform Station, 2021.

[43] Mohammad Sakib Hasan, Jelena Svorcan, Dragoljub Tanovic, Gökçen Baş, and Numan M. Durakbasa. Conceptual Design and Fluid Structure Interaction Analysis of a Solar Powered High-Altitude Pseudo-Satellite (HAPS) UAV Wing Model. pages 93–105. Springer Science and Business Media Deutschland GmbH, 2021. ISBN: 9783030627836. DOI: 10.1007/978-3-030-62784-3_8.

[44] Rudolf Brockhaus, Wolfgang Alles, and Robert Luckner. *Flugregelung*. Springer Berlin Heidelberg, 2011. DOI: 10.1007/978-3-642-01443-7.

[45] Mingjian Wu, Zhiwei Shi, Tianhang Xiao, Z. L.J. Chen, and Haisong Ang. Effect of solar cell efficiency and flight condition on optimal flight control and energy performance for Z-shaped wing stratospheric solar aircraft. *Acta Astronautica*, 164:366–375, 11 2019. ISSN: 00945765. DOI: 10.1016/j.actaastro.2019.08.006.

[46] Mathilde Brizon. Solar Energy Generation Model for High Altitude Long Endurance Platforms, 4 2015.

[47] Ian Moir and Allan G. Seabridge. *Aircraft systems: mechanical, electrical, and avionics subsystems integration*. Wiley, 2008. ISBN: 9780470059968.

[48] Leichtwerk AG. High Altitude Platform Stations (HAPS)-A Future Key Element of Broadband Infrastructure, 2023.

[49] Cristina Beneitez Ortega, Dirk Zimmer, and Patrick Weber. Thermal analysis of a high-altitude solar platform. *CEAS Aeronautical Journal*, 14:243–254, 1 2023. ISSN: 18695590. DOI: 10.1007/s13272-022-00636-9.

[50] FVA. Batteriekühlung: PCM-Simulation. https://www.fva.rwth-aachen.de/2020/01/02/batteriekuehlung/, 2020.

[51] Stemme S10 Retrac variable pitch propeller. https://www.youtube.com/watch?v=pJqJiGkUpvA, 2014.

[52] Stefano Piaquadio, Maximilian Schirp-Schoenen, Mauro Mameli, Sauro Filippeschi, and Kai-Uwe Schröder. Experimental analysis of the thermal energy storage potential of a phase change material embedded in additively manufactured lattice structures. *Applied Thermal Engineering*, 216:119091, 11 2022. ISSN: 1359-4311. DOI: 10.1016/J.APPLTHERMALENG.2022.119091.

[53] Jannik Bühring, Miguel Nuño, and Kai Uwe Schröder. Additive manufactured sandwich structures: Mechanical characterization and usage potential in small aircraft. *Aerospace Science and Technology*, 111:106548, 4 2021. ISSN: 1270-9638. DOI: 10.1016/J.AST.2021.106548.

[54] Joachim Scheiderer. *Angewandte Flugleistung*. Springer Berlin Heidelberg, 2008. DOI: 10.1007/978-3-540-72724-8.

[55] John D. Anderson. *Aircraft performance and design*. WCB/McGraw-Hill, 1999. ISBN: 0070019711.

[56] Andrew J. Keane, Andras Sobester, and James P. Scanlan. *Small Unmanned Fixed-wing Aircraft Design*. Wiley, 2017.

[57] Lukas Girlevicius. Evaluation of solar powered systems in small scale UAV designs, 2022.

[58] Jo Alexander Köhler. Entwurfsmethode für elektrische und hybride Kleinflugzeugantriebe, 2022.

[59] Juan Esteban Gramajo Gonzalez. Assessment of High Altitude and Long Endurance Platforms for Operations in a Commercial Environment, 2016.

[60] André Noth. Design of Solar Powered Airplanes for Continuous Flight (PhD Thesis - Noth 2008), 2008.

[61] Bernhard Keidel. Auslegung und Simulation von hochfliegenden, dauerhaft stationierbaren Solardrohnen, 2000.

[62] Khalilzade Mina Fathi and Prof. S. M. B. Malaek. Wide Area Areal Protective Inspector, 2019.

[63] Hans-Günther Reimerdes. *Auslegung und Struktur von Leichtflugzeugen*. Institut für Strukturdynamik und Leichtbau (RWTH Aachen), 2013.

[64] Mustafa Alp Ertem, Muharrem Altan Akdogan, and Melike Kahya. Intermodal transportation in humanitarian logistics with an application to a Turkish network using retrospective analysis. *International Journal of Disaster Risk Reduction*, 72, 4 2022. ISSN: 22124209. DOI: 10.1016/j.ijdrr.2022.102828.

[65] ADAC Luftrettung gGmbH. ADAC Luftrettung Standorte. https://luftrettung.adac.de/stationen/, 2023. [Online; accessed 09-July-2023].

[66] Joint Chiefs of Staff. Joint Shipboard Helicopter and Tiltrotor Aircraft Operations (JP 3-04), 2012.

[67] Frank Edler Michael Soden René Hankammer. *Fehlerbaumanalyse in Theorie und Praxis Grundlagen und Anwendung der Methode*. 2015. ISBN: 978-3-662-48165-3. DOI: 10.1007/978-3-662-48166-0.

[68] Statistisches Bundesamt. Verbraucherpreisindex in Deutschland von 1991 bis 2022. https://de.statista.com/statistik/daten/studie/2550/umfrage/entwicklung-des-verbraucherpreisindex/, 2023. [Online; accessed 20-December-2023].

[69] M Achternbosch, K.-R Bräutigam, C Kupsch, B Reßler, and G Sardemann. Forschungszentrum Karlsruhe in der Helmholtz-Gemeinschaft Analyse der Umweltauswirkungen bei der Herstellung, dem Einsatz und der Entsorgung von CFK-bzw. Aluminiumrumpfkomponenten, 2003. DOI: 10.5445/IR/270055403.

[70] Deutsche Bahn. DB Strom. https://nachhaltigkeit.deutschebahn.com/de/massnahmen/dbstrom, 2023. [Online; accessed 10-July-2023].

[71] Europäische Kommision. Verordnung des Europäischen Parlaments und des Rates über Batterien und Altbatterien, zur Aufhebung der Richtlinie 2006/66/EG und zur Änderung der Verordnung (EU) 2019/1020. https://eur-lex.europa.eu/legal-content/DE/TXT/HTML/?uri=CELEX:52020PC0798&from=DE, 2020. [Online; accessed 10-July-2023].

[72] Mohan Das, Rinu Chacko, and Susy Varughese. An Efficient Method of Recycling of CFRP Waste Using Peracetic Acid. *ACS Sustainable Chemistry and Engineering*, 6:1564–1571, 2 2018. ISSN: 21680485. DOI: 10.1021/acssuschemeng.7b01456.

[73] José Antonio Butenegro, Mohsen Bahrami, Juana Abenojar, and Miguel Ángel Martínez. Recent progress in carbon fiber reinforced polymers recycling: A review of recycling methods and reuse of carbon fibers. *Materials*, 14, 11 2021. ISSN: 19961944. DOI: 10.3390/ma14216401.

[74] Katsuji Shibata and Mitsutoshi Nakagawa. CFRP Recycling Technology Using Depolymerization under Ordinary Pressure. *Hitachi Chemical Technical Report*, 2014.